

# Self-organized formation of shell-like InAs/GaAs quantum dot ensembles

U.W. Pohl<sup>a,\*</sup>, K. Pötschke<sup>a</sup>, M.B. Lifshits<sup>a,b</sup>, V.A. Shchukin<sup>a,b</sup>,  
D.E. Jesson<sup>c</sup>, D. Bimberg<sup>a</sup>

<sup>a</sup> *Technische Universität Berlin, Institut für Festkörperphysik PN5-2, Hardenbergstr. 36, 10623 Berlin, Germany*

<sup>b</sup> *Abraham Ioffe Physical Technical Institute, St. Petersburg 194021, Russia*

<sup>c</sup> *School of Physics, Monash University, Victoria 3800, Australia*

Available online 19 January 2006

## Abstract

Formation of a multimodal quantum dot (QD) ensemble by strained layer epitaxy of InAs on GaAs near the critical value for the onset of the 2D–3D transition is studied. Reflection anisotropy spectroscopy is employed to confirm that a smooth surface is maintained during strained layer growth prior to QD formation. Instantaneous capping after deposition leads to InAs quantum wells with some thickness fluctuations. Multimodal QD InAs ensembles form after an at least short growth interruption prior to cap layer deposition. The QDs consist of pure InAs with heights varying in steps of complete InAs monolayers. Related exciton energies indicate a simultaneous increase of both height and lateral extension, i.e. a shell-like increase of sizes. The formation of the multimodal QD ensemble is described by a kinetic approach. A growth scenario is presented where QDs having initially shorter base length stop vertical growth at a smaller height, accounting for the experimentally observed shell-like sub-ensemble structure.

© 2006 Elsevier B.V. All rights reserved.

PACS: 81.07.Ta; 81.16.Dn; 81.05.Ea; 81.15.Gh; 78.66.Fd

Keywords: Quantum dot formation; Multimodal distribution

## 1. Introduction

Strained layer heteroepitaxy has evolved as a major method to fabricate self-organized quantum dots (QDs) of high structural quality [1]. The luminescence of such QD ensembles is inhomogeneously broadened due to size or composition variations around an average. A breakdown of the broad ensemble luminescence into up to eight well-separated peaks was recently observed and, by comparison to k·p model calculations, unambiguously assigned to sub-ensembles of flat, shell-like InAs QDs with heights varying in steps of complete InAs monolayers [2–4]. Details of the formation of such ensembles were not yet reported. We present experimental data on the early stage of multimodal QD ensemble

formation and a kinetic description of a possible formation scenario.

## 2. Experimental procedure

Strained In(Ga)As layers were grown on homoepitaxial GaAs buffers in a horizontal MOCVD reactor equipped with a low-strain quartz window, using TMin, TMGa, and TBAs precursors [2]. The optical response to actual growth processes was monitored recording in situ the reflection anisotropy spectra (RAS), i.e. the difference in reflectance measured along the two surface symmetry axes  $[\bar{1}10]$  and  $[110]$  [5]. Multimodal QD ensembles were obtained from InAs layers deposited with a comparably large growth rate of 0.4 monolayers/s (ML/s) at 490 °C and a thickness close to the critical value for surface faceting in the Stranski–Krastanow (SK) growth mode. A growth interruption (GRI) without precursor supply was applied prior to GaAs cap layer deposition to allow for QD formation and ripening. For photoluminescence (PL)

\* Corresponding author. Tel.: +49 30 314 24239; fax: +49 30 314 22064.

E-mail address: [pohl@physik.tu-berlin.de](mailto:pohl@physik.tu-berlin.de) (U.W. Pohl).

studies QD emission was excited at 514.5 nm and detected by a cooled Ge diode.

### 3. Experimental results

Perceptibility of multimodal InAs QD sub-ensembles in PL spectra requires well-defined sharp upper and lower interfaces to GaAs. A sharp *lower* interface is easily achieved by a smooth GaAs surface [6]. To obtain information on the *upper* interface, we first characterize the deposition on smooth GaAs surfaces using RAS. In a second step, InAs is deposited with varying growth interruptions prior to cap layer growth.

#### 3.1. Control of In(Ga)As deposition

In(Ga)As layers with thicknesses below and just above the critical value for elastic relaxation were studied in situ by recording transients of the RAS signal at a fixed photon energy. An energy of 2.6 eV was selected due to its high surface sensitivity [7]. The SK transition was retarded by the Ga composition to reduce the strain in the layers. This allowed for optically tracing the response of strained layers. The RAS transients of such InGaAs/GaAs layers show oscillations, which are particularly pronounced at high Ga composition, cf. Fig. 1. The oscillations originate from reconstruction domains of reduced As coverage close to monolayer steps [8], which occur in the island growth mode at the low deposition temperature used for QD growth. The damping of the modulation for increasing In content is attributed to a combined effect of a more group-III-rich surface due to reduced As–In bond strength as compared to As–Ga, and that of a transition to step-flow growth due to the higher surface mobility of In

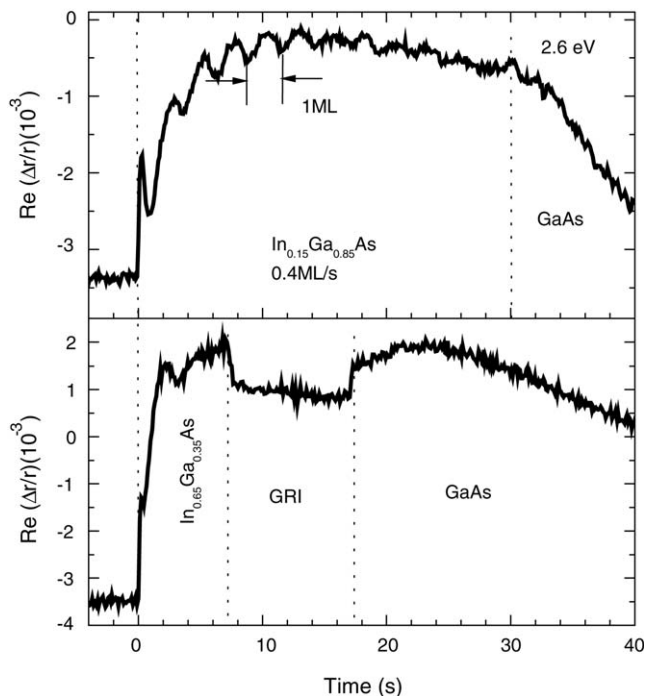


Fig. 1. RAS transients recorded at 2.6 eV during deposition of InGaAs/GaAs layers with varied In composition at 485 °C.

species as compared to Ga. At 50% Ga content the oscillation disappears after about three monolayers. Overcritical layers with 65% Ga show just two monolayer oscillations. QD formation does not lead to a clear feature in the response. The apparent drop of the signal is related to the stop of precursor supply during GRI. The RAS response during GRI basically originates from the In(Ga)As wetting layer, the slow changes are assigned to an optically detected coarsening due to QD ripening. The in situ RAS study demonstrates that a smooth growth front is maintained during strained layer deposition on GaAs prior to QD formation.

#### 3.2. Characteristics of InAs layers

To induce multimodal QD formation,  $\sim 1.9$  ML thick InAs layers were deposited. This thickness just exceeds the critical value for a SK transition. The growth interruption prior to cap layer deposition has a strong effect on the structural and optical properties of the layers. PL spectra of samples grown with varying GRIs are given in Fig. 2. The narrow PL of a sample grown *without* GRI corresponds to an  $e_0$ - $hh_0$  exciton recombination in a pseudomorphic InAs/GaAs quantum well (QW) of  $\sim 1.8$  ML thickness, in good agreement with the amount of deposited material. The apparent asymmetry at the low-energy side is well described by an exponential function  $I \sim \exp(E/E_0)$ . This behavior indicates QW states with a DOS tail originating from potential fluctuations due to thickness or alloy variations [9]. The characteristic energy for the studied emission is  $E_0 = 12.3$  meV. Recent TEM studies proved that no intermixing occurred under the given growth conditions [4]. The PL hence proves the formation of an InAs/GaAs quantum well with a residual roughness if no GRI is applied.

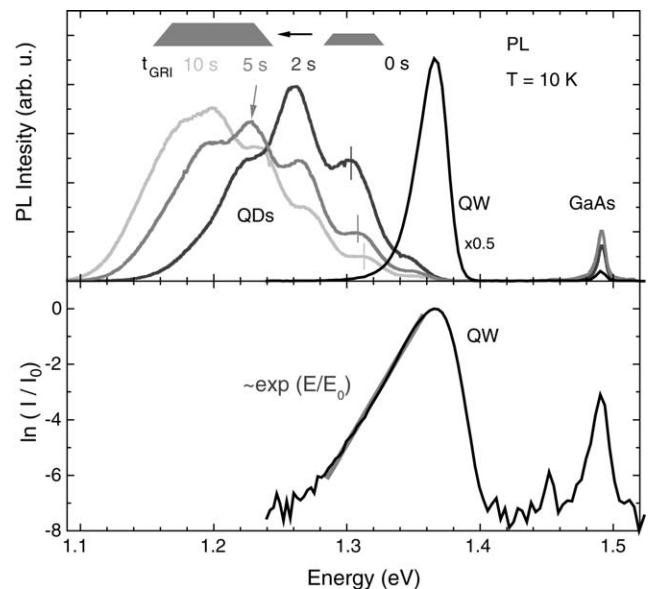


Fig. 2. Top: PL spectra of InAs/GaAs layers grown with varied durations  $t_{\text{GRI}}$  of a growth interruption prior to GaAs cap layer deposition. The scheme on top illustrates the shell-like QD size increase. Bottom: Semilogarithmic plot of the spectrum from the sample grown without growth interruption (black curve) and description of the low energy tail by an exponential function (grey line).

### 3.3. Multimodal InAs QD ensembles

Samples grown with an additional GRI clearly show PL of multimodal QD ensembles (Fig. 2). QDs hence form *after* InAs deposition. The emission of the wetting layer appears at increased excitation intensity (not shown). The red-shift of the ensemble PL energy found for increased GRI indicates an average QD size increase. Note that the individual sub-ensembles do *not* shift to the red. Detailed calculation of the exciton transition energies of InAs/GaAs QDs with truncated pyramidal shape showed that an increase in height generally is accompanied by a simultaneous increase of the base length, resulting in a *shell-like* growth from one sub-ensemble to the next [3]. For longer GRI, the peak of a given sub-ensemble shifts to the *blue* as indicated by bars on the maxima near 1.3 eV. Furthermore, the complete distribution tends to get asymmetric with a tail on the high energy side, i.e. at sub-ensembles of small QDs. Both features indicate that the evolution proceeds by a dissolution of sub-ensembles of smaller QDs to form sub-ensembles of larger QDs. The dissolution of smaller QDs at a time proceeds essentially by a decrease of QD height. The minor lateral shrinking is indicated by the small magnitude of the blueshift of individual sub-ensembles mentioned above. PLE studies demonstrated that thickness and composition of the wetting layer remains constant during this process and can be described by 1 ML pure InAs [4].

## 4. Kinetic description of multimodal QD ensemble formation

To describe theoretically the formation of an ensemble of strained InAs islands with an InAs wetting layer on GaAs substrate during GRI, we assume square base islands with a truncated pyramidal shape. The islands are surrounded by the adatom sea and grow or dissolve by attaching or detaching adatoms.

### 4.1. Scenario for the formation of a multimodal QD distribution

The evolution process is strongly affected by a stress maximum at the base perimeter of the strained islands, leading to a logarithmic singularity in the elastic energy density creating a barrier for the formation of a new atomic layer on a side facet [10]. The barrier strength increases upon the island height for a given base length. At the initial state, the system consists of flat, 1 ML high islands on the WL with a broad distribution in base lengths. These islands can grow in both base length and height. As 2 ML high islands form, the barrier strength increases hindering further island growth in base length. Further growth will then occur preferably via monolayer nucleation on the top facet. The island base then remains constant and the height increases by one monolayer after another. Different sub-ensembles of islands having different initial island bases evolve independently. The energetics of the growth of every next atomic layer atop a given truncated pyramid is described by a change of the Gibbs free energy of the

system due to the formation of an embryo which partially covers the top facet

$$\delta\Phi_{\text{island}} = \delta E_{\text{edge}} + \delta E_{\text{elast}} - \mu\delta N, \quad (1)$$

$\delta E_{\text{edge}}$  being the step energy of the embryo edge,  $\mu$  the adatom sea chemical potential, and  $\delta N$  the number of atoms in the embryo. The elastic relaxation energy change  $\delta E_{\text{elast}}$  can be found by using the small slope approximation [11]. Initially  $\delta\Phi_{\text{island}} > 0$  as the embryo formation starts. If the embryo exceeds some critical size,  $\delta\Phi_{\text{island}}$  becomes negative so that the embryo formation lowers the system free energy, cf. Fig. 3. Since the island has the shape of a truncated pyramid, the size of the top facet decreases during growth of one monolayer after the next. At a certain height, the top size is no longer large enough to favor the formation of the next embryo. Growth of this island will then stabilize at this size. Islands with larger initial bases have larger top sizes at the same height, such islands will therefore stabilize at a larger height.

### 4.2. Modeling of the multimodal distribution formation

The ensemble evolution model considers elementary processes of the growth of an island having a base  $L$  and a height  $h$  by an increase of the height by 1 ML ( $h \rightarrow h + 1$ ) or partial dissolution of an island ( $h \rightarrow h - 1$ ). The processes described by rate equations involve overcoming a barrier which obey the Arrhenius dependence [12]

$$W(L, h \rightarrow h \pm 1) = \omega \exp \frac{-\delta\Phi_{\text{barrier}}}{k_B T}, \quad (2)$$

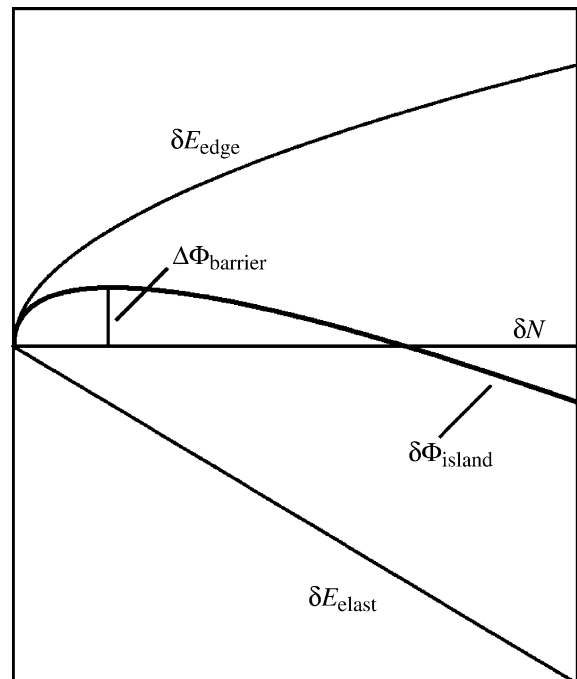


Fig. 3. Gibbs free energy change  $\delta\Phi_{\text{island}}$  due to the formation of a monolayer embryo on the top facet of a QD and its contributions.

assuming the same prefactor  $\omega$  for all islands. The temporal evolution of the distribution function  $P(L, h; t)$  obeys the master equation

$$\begin{aligned} \frac{\partial P(L, h; t)}{\partial t} = & W(L, h-1 \rightarrow h) \times P(L, h-1; t) \\ & - W(L, h \rightarrow h-1) \times P(L, h; t) \\ & - W(L, h \rightarrow h+1) \times P(L, h; t) \\ & + W(L, h+1 \rightarrow h) \times P(L, h+1; t). \end{aligned} \quad (3)$$

The growth or dissolution of the islands proceeds by mass exchange between the islands and the adatom sea. For the growth interruption, the mass conservation law reads

$$q_{\text{adatom}}(t) + \sum_L \sum_h P(L, h; t) V(L, h) = Q = \text{const}, \quad (4)$$

where the island volume  $V(L, h)$  is counted in number of atoms,  $q_{\text{adatom}}$  is the surface concentration of adatoms on the WL, and  $Q$  is the excess amount of the deposited material exceeding the critical WL thickness. The adatom concentration is related to the adatom sea chemical potential

$$q_{\text{adatom}} = \exp \frac{\mu}{k_B T}. \quad (5)$$

As the islands start growing, the number of adatoms in the adatom sea decreases, thereby lowering the chemical potential  $\mu$ . The latter results in a larger critical embryo size, and the limiting heights of the islands become smaller. This additionally contributes to stop the island growth.

A sample result of the solution of the coupled set of Eqs. (3)–(5) is shown in Fig. 4. Starting from a broad distribution ( $L = 25 \cdot \cdot 33$ ) of flat islands ( $h = 2$ ), the initial distribution evolves via a predominantly vertical growth with a fixed base into a final distribution of 3D islands, where islands with larger bases have also a larger height. The result reproduces specific features of the experimental data. First, the particular island distribution in base

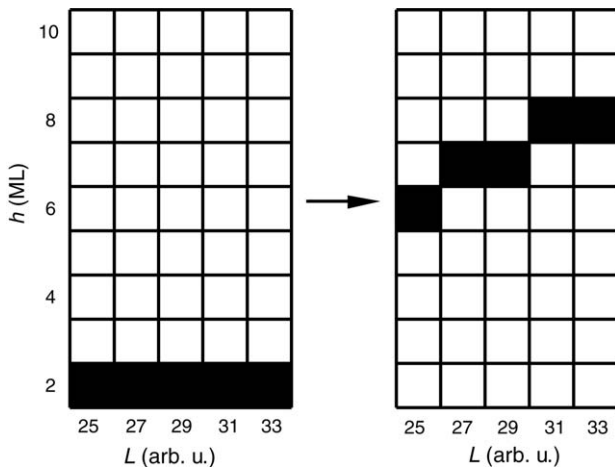


Fig. 4. Schematics of an island ensemble distribution evolving in base length  $L$  and height  $h$  from an initial state of flat islands with various lengths to a multimodal final state.

length and height is described. Second, a temporal evolution of the PL spectra upon growth interruption, where the intensity of each peak corresponding to a certain island height  $h$  first increases and then decreases. This is due to the fact that islands with many different base lengths first reach the height  $h$  and then the islands with larger base length grow in height further. Third, the small blueshift of the individual sub-ensemble PL peaks with time may be explained similarly; for a given height  $h$ , islands with larger bases grow further in height and remaining islands with smaller bases shift the PL peak to higher photon energies.

## 5. Conclusion

Multimodal InAs QD ensembles form on GaAs substrates from strained layers with a thickness near the critical value for the onset of 3D island formation. Reflection anisotropy spectroscopy shows that the initial smooth surface is maintained during heteroepitaxy. Immediate capping after deposition leads to InAs quantum wells with some thickness fluctuations. Multimodal QD InAs ensembles form after an at least short growth interruption prior to cap layer deposition. In the framework of a kinetic description for the formation of a multimodal QD ensemble, a growth scenario is presented where QDs having initially shorter base lengths stop vertical growth at a smaller height. The approach accounts for the experimentally observed shell-like sub-ensemble structure.

This work was supported by the Deutsche Forschungsgemeinschaft in the framework of SFB 296, the SANDiE Network of Excellence of the European Commission, the Russian Foundation for Basic Research RFBR, and by the Russian Federal Program on Support of Leading Scientific Schools.

## References

- [1] D. Bimberg, M. Grundmann, N.N. Ledentsov, *Quantum Dot Heterostructures*, Wiley, Chichester, 1999.
- [2] K. Pötschke, L. Müller-Kirsch, R. Heitz, R.L. Sellin, U.W. Pohl, D. Bimberg, N. Zakharov, P. Werner, *Physica E* 21 (2004) 606.
- [3] R. Heitz, F. Guffarth, K. Pötschke, A. Schliwa, D. Bimberg, N.D. Zakharov, P. Werner, *Phys. Rev. B* 71 (2005) 045325.
- [4] U.W. Pohl, K. Pötschke, A. Schliwa, F. Guffarth, D. Bimberg, N.D. Zakharov, P. Werner, M.B. Lifshits, V.A. Shchukin, D.E. Jesson, *Phys. Rev. B* 72 (2005) 245332.
- [5] D.E. Aspnes, J.P. Harbison, A.A. Studna, L.T. Florez, *J. Vac. Sci. Technol. A* 6 (1988) 1327.
- [6] R. Sellin, F. Heinrichsdorff, Ch. Ribbat, M. Grundmann, U.W. Pohl, D. Bimberg, *J. Cryst. Growth* 221 (2000) 581.
- [7] U.W. Pohl, K. Pötschke, I. Kaiander, J.-T. Zettler, D. Bimberg, *J. Cryst. Growth* 272 (2004) 143.
- [8] J.-T. Zettler, J. Rumberg, K. Ploska, K. Stahrenberg, M. Pristovsek, W. Richter, M. Wassermeier, P. Schützendübe, J. Behrend, L. Däweritz, *Phys. Stat. Sol. (a)* 152 (1995) 35.
- [9] M. Oueslati, M. Zouaghi, M.E. Pistol, L. Samuelson, H.G. Grimmeiss, M. Balkanski, *Phys. Rev. B* 32 (1985) 8220.
- [10] D.E. Jesson, G. Chen, K.M. Chen, S.J. Pennycook, *Phys. Rev. Lett.* 80 (1998) 5156.
- [11] J. Tersoff, R.M. Tromp, *Phys. Rev. Lett.* 70 (1993) 2782.
- [12] M.B. Lifshits, V.A. Shchukin, D. Bimberg, D.E. Jesson, *Proceedings of the 13th International Symposium on Nanostructures: Physics and Technology*, St. Petersburg, Russia, 2005. (Ioffe Physico-Technical Institute, St. Petersburg, 2005), pp. 308–309.